Bioconjugate Chemistry

Article

pubs.acs.org/bc

Flow and Microwave-Assisted Synthesis of *N*-(Triethylene glycol)glycine Oligomers and Their Remarkable Cellular Transporter Activities

ThingSoon Jong, Ana M. Pérez-López, Emma M. V. Johansson, Annamaria Lilienkampf, and Mark Bradley*

School of Chemistry, EaStCHEM, University of Edinburgh, Joseph Black Building, King's Buildings, West Mains Road, EH9 3FJ Edinburgh, United Kingdom

Supporting Information

ABSTRACT: Peptidomimetics, such as oligo-*N*-alkylglycines (peptoids), are attractive alternatives to traditional cationic cell-penetrating peptides (such as R_9) due to their robust proteolytic stability and reduced cellular toxicity. Here, monomeric *N*-alkylglycines, incorporating amino-functionalized hexyl or triethylene glycol (TEG) side chains, were synthesized via a three-step continuous-flow reaction sequence, giving the monomers *N*-Fmoc-(6-Boc-aminohexyl)glycine and *N*-Fmoc-((2-(2-Boc-aminoethoxy)ethoxy)ethyl)glycine in 49% and 41% overall yields, respectively. These were converted into oligomers (5, 7, and 9-mers) using an Fmoc-based solid-phase protocol and evaluated as cellular transporters. Hybrid oligomers, constructed of alternating units of the aminohexyl and amino-TEG monomers, were non-cytotoxic and exhibited remarkable cellular uptake activity compared to the analogous fully TEG or lysine-like compounds.

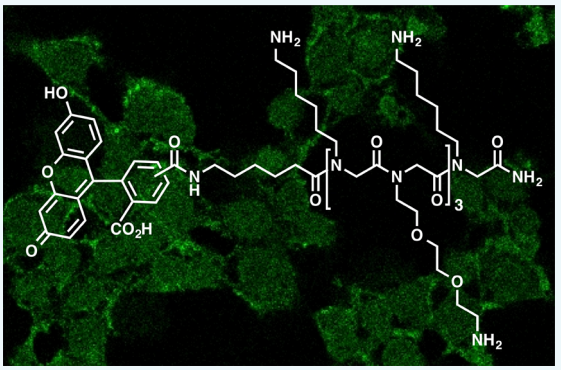

INTRODUCTION

Cellular delivery of chemical and biological cargos is of great importance in biology and medicine;[1−3] however, cellular access is often limited by cargo solubility and physico−chemical properties.[4,5] To overcome these problems, a number of cellular delivery techniques have been developed,[6−9] including the use of protein-derived cell-penetrating peptides[10−12] (CPPs) such as those based on Tat_{49-57},[12,13] Penetratin,[14] and Transportan.[15] CPPs are capable of translocating across the cell membrane due to their interaction with the plasma membrane, with a host of mechanistic uptake possibilities hypothesized: including endocytosis, direct translocation, and "surface rafts".[16−18] Polylysines and polyarginines have been shown to increase cellular uptake of a number of molecules (e.g., methotrexate and cyclosporine A),[19,20] with the 9-mer of L-arginine and D-arginine reportedly being 20- and >100-fold more efficient than HIV Tat_{49-57}, respectively.[21]

Although the aforementioned CPPs work relatively well, they can suffer from cytotoxicity (a common issue with polyguanidinium motifs) and cargos often remain trapped in endosomes.[22] In order to improve cellular delivery alongside increased serum stability, peptidomimetics such as oligo-*N*-alkylglycines (commonly referred to as peptoids) have been investigated as alternatives to traditional CPPs.[23−28] Peptoids offer structural flexibility due to the absence of chirality and hydrogen bond donors on their backbone, while the presence of the tertiary amides decreases the polarity of the oligomer, therefore restricting the formation of secondary structures based on backbone hydrogen bonding.[29,30] Cationic peptoids have highly efficient cell delivery profiles and are nontoxic in vivo,[31−33] making them attractive candidates for cellular delivery.

Peptoids are typically synthesized via solid-phase synthesis using *N*-substituted *N*-Fmoc-glycine monomers in an Fmoc/^{t}Bu type strategy.[34,35] However, this "monomer" approach requires the multistep synthesis of *N*-Fmoc-glycine monomers, which are conventionally performed in batch. Flow chemistry[36−38] enables the integration of individual synthetic steps into a linear sequence to improve productivity and synthetic efficiency.[39−43] This is mainly due to improved physical transport phenomena during chemical reactions as a result of the intrinsic properties of flow reactors (10−1000 μm inner dimensions).[44−46] Recently, we reported the efficient flow-mediated synthesis of Boc, Fmoc, and Dd*iv* monoprotected aliphatic diamines, highlighting enhanced reaction selectivity in a tubular flow reactor.[47]

Here, in order to improve the efficiency of peptoid synthesis, a scalable continuous flow procedure for the monomer *N*-Fmoc-(6-Boc-aminohexyl)glycine **1** and its triethylene glycol (TEG) analogue *N*-Fmoc-((2-(2-Boc-aminoethoxy)ethoxy)-

Received: June 1, 2015
Revised: June 30, 2015

DOI: 10.1021/acs.bioconjchem.5b00307
Bioconjugate Chem. XXXX, XXX, XXX−XXX

Chart 1. "Hybrid" (H5, H7, and H9), TEG (T5, T7, and T9), and "Lysine-Like" (L5, L7, and L9) Peptoids, and the Structure of the Monomers, *N*-Fmoc-(6-Boc-aminohexyl)glycine 1 and *N*-Fmoc-((2-(2-Boc-aminoethoxy)ethoxy)ethyl)glycine 2, Used in Their Solid-Phase Synthesis[a]

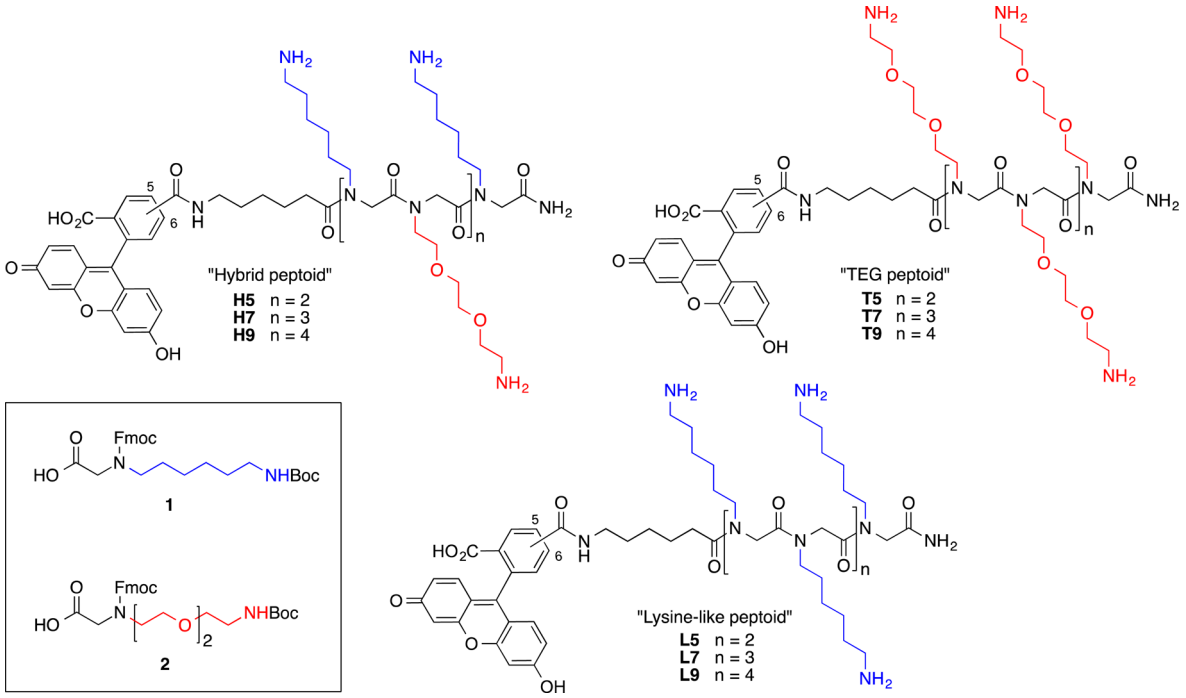

[a]The peptoids were synthesized and isolated as a mixture of 5(6)-isomers of carboxyfluorescein.

ethyl)glycine **2** is reported. These two monomers were used to synthesize a new class of "hybrid peptoids", constructed from alternating units of the aminohexyl and amino-TEG based monomers **1** and **2**, with a focus on optimizing cellular uptake (Chart 1). It is known that the amphiphilicity of typically highly cationic peptoids influences their cell permeability and subcellular localization,[48,49] and the current designs of new cellular transporters involves achieving a delicate balance between hydrophilic and hydrophobic structural components.[50−52] Here, the TEG moiety was introduced as a peptoid side chain to improve solubility, hence potentially enhancing their cellular uptake.[53−55] These new "hybrid peptoids" (**H5**, **H7**, and **H9**) showed significantly increased cellular uptake compared to the traditional lysine-like peptoids (**L5**, **L7**, and **L9**).

RESULTS AND DISCUSSION

The monomer *N*-Fmoc-(6-Boc-aminohexyl)glycine **1**, which is used to synthesize the lysine-like peptoids, is typically synthesized in batch from 1,6-diaminohexane in four steps.[34] Mono-Boc protection of 1,6-diaminohexane with Boc_2O gives *N*-Boc-1,6-diaminohexane **3**, which is followed by *N*-alkylation with benzyl 2-bromoacetate to give benzyl 2-[(6-{[(*tert*-butoxy)carbonyl]amino}hexyl)amino]-acetate **4**. Fmoc carbamation of the secondary amine in **4** with Fmoc-OSu (to give **5**) and subsequent catalytic hydrogenolysis gives monomer **1**. A key challenge of this route is to achieve a high degree of reaction selectivity for the first two steps, which can be hard to achieve in conventional batch synthesis due to system inhomogeneity. Similarly, the hydrogenolysis of the benzyl protecting group in **5** can be adversely affected by a competing side reaction resulting in cleavage of the Fmoc group.[56,57]

Continuous Flow Synthesis of Peptoid Monomers. The four-step flow synthesis of the peptoid monomers **1** and **2** was adapted from the batch route and performed in a self-assembled flow system, which incorporated PTFE tubular reactors, packed scavengers, and catalyst (SI, Figure S1). Monomer **1** was used as an optimization target and the developed route was applied to the synthesis of the TEG monomer **2**. As reported previously, the mono-Boc carbamation of 1,6-diaminohexane under flow conditions gave the monoprotected product **3** in 61% yield,[47] which was used as a building block in a series of flow reactions. The next two steps, monoalkylation and Fmoc carbamation, were linked into a tandem sequence using in-line scavengers, followed by a transfer hydrogenolysis using an immobilized Pd catalyst.

Flow Mediated Monoalkylation and Fmoc Carbamation. Alkylation of **3** with 1 equiv of benzyl 2-bromoacetate was explored by varying the concentration, solvent, and base (Table 1). The residence time and temperature were set at 3 min and 100 °C, respectively; as a preliminary screen showed that a longer residence time (5 min) resulted in a lower conversion to **4**, and a temperature range between 90 and 100 °C was well tolerated (SI, Figure S2). The highest conversion to monoalkylated **4** (85%) was observed using 40 mM of **3** and 3.0 equiv of DIPEA in MeCN (working pressure <2 bar). Changing the solvent to DMF reduced both the conversion to **4** and the monoselectivity of the reaction (entries a vs b, Table 1), as did replacing DIPEA with piperidine (PIP), DBU, or TEA (DBU and PIP gave dismal conversion) (entries c−e, Table 1). A lower conversion (70% and 69%, respectively) was detected at a higher reactant concentration (entry g, Table 1) and when the starting materials were not preheated before mixing (entry f, Table 1), emphasizing the importance of reactant preconditioning.

DOI: 10.1021/acs.bioconjchem.5b00307
Bioconjugate Chem. XXXX, XXX, XXX−XXX

Table 1. Optimization of the Flow-Mediated Mono-Alkylation Reaction of *N*-Boc-1,6-diaminohexane.[a]

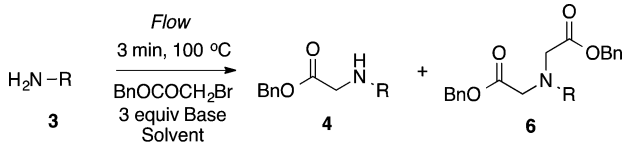

entry	solvent	base	conc 3	4[b] (%)	ratio 4:6[c]
a	DMF	DIPEA	40 mM	69	1:0.16
b	MeCN	DIPEA	40 mM	85	1:0.10
c	MeCN	PIP	40 mM	6	–
d	MeCN	DBU	40 mM	10	–
e	MeCN	TEA	40 mM	69	1:0.06
f[d]	MeCN	DIPEA	40 mM	69	1:0.08
g	MeCN	DIPEA	100 mM	70	1:0.11

[a]20 μmol scale, 1 equiv of benzyl 2-bromoacetate, flow rate 0.67 mL/min. [b]Average conversion measured by HPLC with UV detection at 254 nm (n = 3, variation in conversions within ±3%), with methyl benzoate used as an internal standard. [c]Integrated peak ratio of **4** to **6**. [d]No preheating of reactants before mixing.

The single step Fmoc carbamation of **4** was achieved at room temperature using 1.0 equiv of Fmoc-Cl (both reagents at 20 mM in MeCN) with a residence time of 3 min to give the Fmoc-protected benzyl acetate **5** in 98% isolated yield. Fmoc-Cl was chosen due to its better reactivity compared to Fmoc-OSu, especially with sterically hindered secondary amines.[58]

Using the optimized parameters for the alkylation and Fmoc carbamation reactions, the two steps were joined into a cascading flow sequence. The unreacted alkylating reagent from the first reaction stream was removed prior to the Fmoc carbamation step by directly connecting the exiting stream from the alkylation reaction of **3** (immediately after the back-pressure regulator) to a scavenging column (6.0 × 0.5 cm), packed with 0.6 g of Trisamine-Si (loading 1.58 mmol/g). Based on HPLC analysis, Trisamine-Si was more effective in removing excess benzyl 2-bromoacetate than Thiol-Si scavengers. After the scavenging column, the reaction stream was cooled to room temperature prior to the mixing of **4** with Fmoc-Cl. Here, 15 mM of Fmoc-Cl (1.2 equiv) in MeCN was used, the concentration adjusted based on the 85% conversion into **4** during the first reaction step. With a residence time of 3 min for both reactions, 4.9 mmol of **3** gave a 69% isolated yield of **5** over two steps (Scheme 1).

Flow Mediated Catalytic Transfer Hydrogenolysis. The final step of the monomer synthesis was the catalytic hydrogenolysis of the benzyl ester moiety to give the corresponding carboxylic acid. Batch synthesis of **1** demonstrated that the Fmoc protecting group in **5** is (partially) labile toward Pd-catalyzed hydrogenolysis, resulting in a mixture of products depending on the reaction conditions and activity of the catalyst. The facile manipulation of contact time between the active catalyst and the substrate in a flow system was expected to promote reaction selectivity and thus reduce the occurrence of the Fmoc deprotection. With the aim of improving the scope of hydrogenolysis reactions in flow, the transfer hydrogenolysis strategy was chosen over the more commonly used H_2. Flow transfer catalytic hydrogenolysis of **5** was achieved by passing the reactants through an immobilized catalyst (3.0 × 0.4 cm, loading ∼150 mg/cartridge), with the reaction screened for the optimal catalyst, substrate concentration, and temperature, using 2.5 equiv of 1,4-cyclohexadiene as the hydrogen donor. The use of ammonium formate as a hydrogen donor was incompatible with the flow system resulting in fluctuations of operating pressure. Four different catalysts (10% Pd/C, 20% $Pd(OH)_2/C$, 5% Pt/C, and 5% Ru/Al_2O_3) and three substrate concentrations (15, 30, and 50 mM) were tested (Table 2). 10% Pd/C as a catalyst required heating to 40 °C to give good conversion to **1** with 15 mM being the optimal reactant concentration (entry b, Table 2); however, at the elevated temperature, conversion to the Fmoc deprotected side product **7** was also observed (entries b–d, Table 2). Furthermore, this catalyst proved unsuitable for larger-scale reactions (3.4 mmol of **5**) as saturation of the cartridge was observed after 20 min (∼14% of total reaction progress) along with unstable working pressures (fluctuating between 9 and 11 bar).

Pearlman's catalyst (20% $Pd(OH)_2/C$) produced the best results with ≥70% conversion across the whole range of

Scheme 1. Continuous Flow Synthesis of *N*-Fmoc-(6-Boc-aminohexyl)glycine 1 and *N*-Fmoc-((2-(2-Boc-aminoethoxy)ethoxy)ethyl)glycine 2[a]

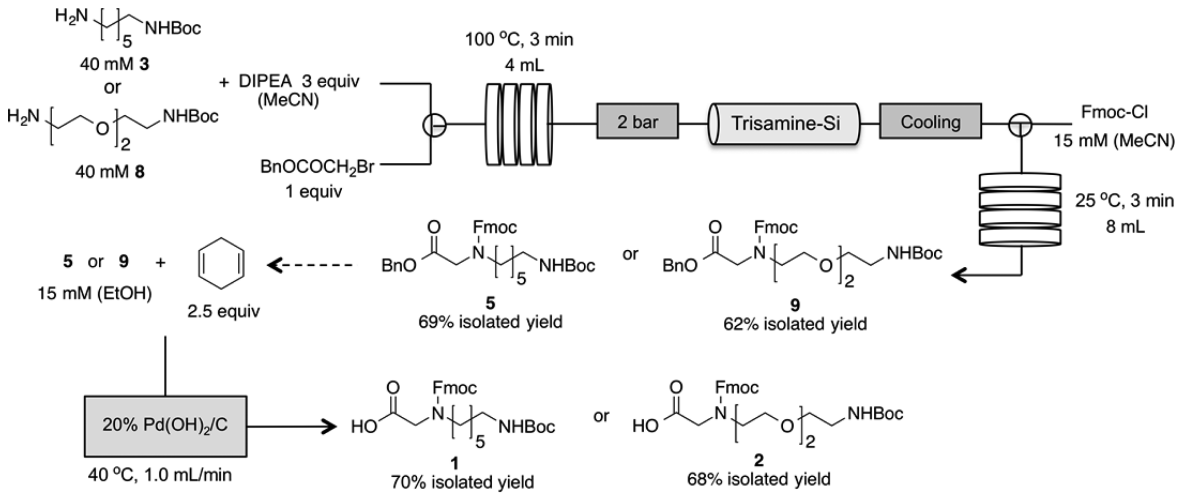

[a]The continuous flow protocol was completed in three key steps with 49% and 41% overall yields for **1** and **2**, respectively.

DOI: 10.1021/acs.bioconjchem.5b00307
Bioconjugate Chem. XXXX, XXX, XXX–XXX

Table 2. Catalyst Screening for the Flow-Mediated *O*-Bn Hydrogenolysis[a]

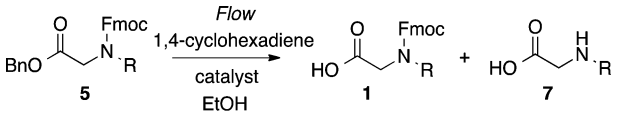

entry	catalyst	5 (mM)	temp (°C)	1[b] (%)	ratio[c] 1:7
a	10% Pd/C	15	rt	23	nd
b	10% Pd/C	15	40	78	1:0.25
c	10% Pd/C	30	40	69	1:0.15
d	10% Pd/C	50	40	54	1:0.10
e	20% $Pd(OH)_2/C$	15	40	96	1:0.00
f	20% $Pd(OH)_2/C$	30	40	82	1:0.08
g	20% $Pd(OH)_2/C$	50	40	70	1:0.10
h	5% Pt/C	15	40	–	–
i	5% Ru/Al_2O_3	15	40	–	–

[a]7.5 μmol scale, 2.5 equiv 1,4-cyclohexadiene, flow rate 1 mL/min. [b]Average conversion measured by HPLC with UV detection at 254 nm (n = 3, variation in conversions within ±3%), with aniline used as an internal standard. [c]Integrated peak ratio of **1** to **7**.

substrate concentrations tested (15−50 mM). At 15 mM of **5**, no Fmoc cleavage was detected with 96% conversion to **1** (entry e, Table 2) along with a low and stable system pressure (1 bar). For both Pd catalysts, reduced conversion was observed as the concentration of substrate was increased from 15 to 50 mM. 5% Pt/C and 5% Ru/Al_2O_3 were unsuccessful in flow transfer hydrogenolysis despite their ability to promote the debenzylation process in batch chemistry.[59] Using 20% $Pd(OH)_2/C$ and 2.5 equiv of 1,4-cyclohexadiene, the hydrogenolysis of monomer **1** was achieved in 70% isolated yield (overall yield 49% over three steps) (Scheme 1). The combined reaction time (~10 h, excluding purifications) required to synthesize **1** by this flow method was approximately four times faster than that typically required for the corresponding batch method.

Based on the optimized continuous flow procedures for monomer **1**, the TEG-based monomer **2** was synthesized using the same experimental setup using mono-Boc protected 2,2′-(ethylenedioxy)bis(ethylamine)[47] **8** as the starting material. The alkylation and Fmoc-carbamation sequence (4.9 mmol scale) gave the protected intermediate **9** (62% isolated yield) and the subsequent debenzylation produced monomer **2** in 68% yield (41% overall yield over three steps) (Scheme 1). The synthetic yields for the TEG monomer **2** were comparable to the yields obtained with the lysine-like monomer **1**, thus demonstrating the consistency of the continuous flow protocol.

Design and Synthesis of Hybrid Peptoids. In an effort to correlate the cellular penetration efficiency of molecular transporters with their structural characteristics, new cationic "hybrid peptoids", featuring an alternating sequence of monomers **1** and **2**, were synthesized and compared to lysine-like peptoids and to peptoids constructed solely from TEG-monomer **2**. Three different oligomer lengths (5-, 7-, and 9-mer) of each peptoid type were synthesized to allow direct comparison of their cellular uptake.

The hybrid peptoids **H5**, **H7**, and **H9** and TEG peptoids **T5**, **T7**, and **T9** were synthesized on a Rink-amide functionalized aminomethyl polystyrene resin (1% DVB, 100−200 mesh, loading 1.23 mmol/g) using the Fmoc/^{t}Bu-strategy with DIC/Oxyma as coupling reagents (SI, Scheme S1). The synthesis of

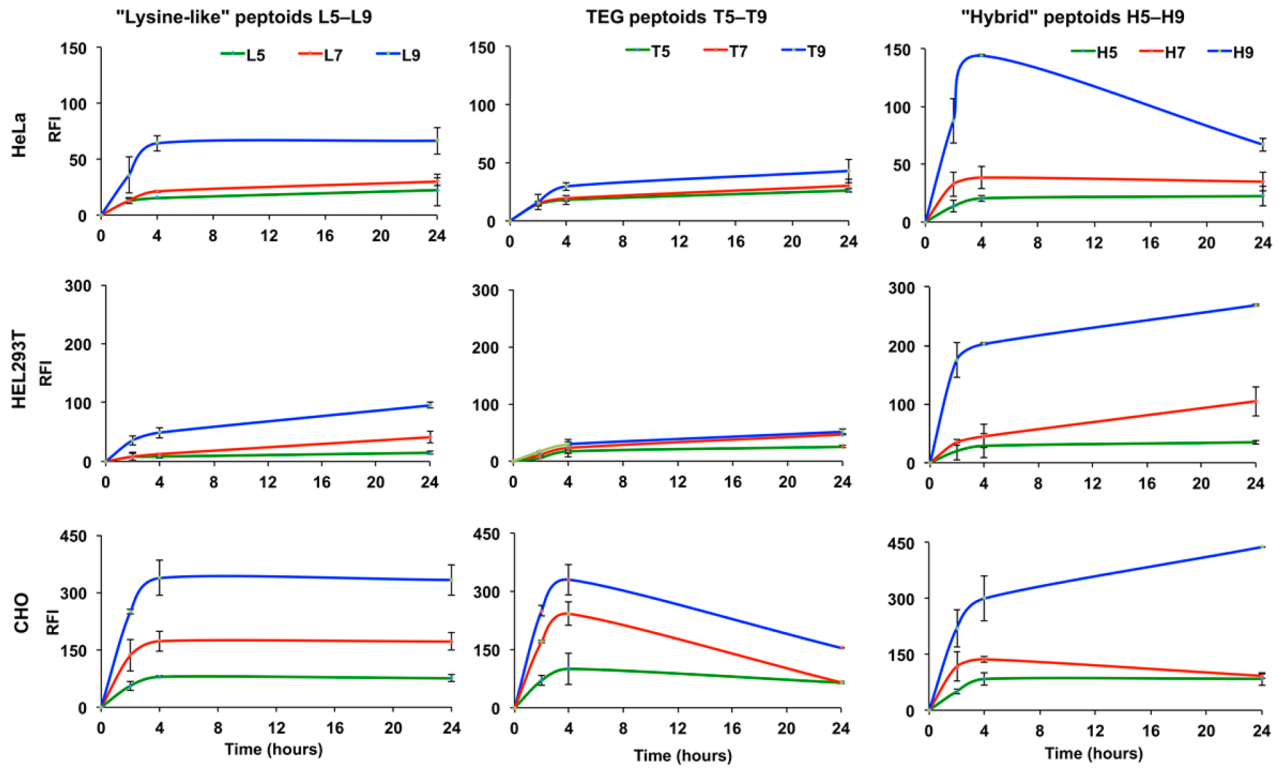

Figure 1. Time-dependent cellular uptake of lysine-like, TEG, and hybrid peptoids in HeLa, HEK293T, and CHO cells (y-axis represents relative fluorescence intensity (RFI) and x-axis incubation time in hours). The cells were incubated with 10 μM of each peptoid for 2, 4, and 24 h at 37 °C (n = 3) and fluorescence intensity measured by flow cytometry ($\lambda_{Ex}/\lambda_{Em}$ 488/530 nm). Prior to the analysis, the samples were treated with Trypan Blue to quench extracellular fluorescence.

DOI: 10.1021/acs.bioconjchem.5b00307
Bioconjugate Chem. XXXX, XXX, XXX−XXX

peptoids **T5**, **T7**, and **T9**, containing only the TEG-based monomer **2**, proved challenging with the coupling reactions requiring microwave (μw) heating at 75 °C for 25 min. Similarly, the subsequent Fmoc deprotection steps (20% PIP in DMF) with **T5**, **T7**, and **T9** required μw heating at 60 °C (2 × 10 min). The same μw assisted deprotection procedure was successful with the hybrid peptoids **H5**, **H7**, and **H9** up to heptamer sequences on the resin, after which the Fmoc deprotection required treatment with DBU−PIP (2% DBU and 2% PIP in DMF for 60 °C μw for 10 min, followed by 4% DBU and 4% PIP for 10 min). The lysine-like peptoids **L5**, **L7**, and **L9** were synthesized in similar fashion with deprotection at room temperature using 20% PIP in DMF (2 × 10 min).[34] 6-Aminohexanoic acid (εAhx) as a spacer and 5(6)-carboxyfluorescein were consecutively coupled to the *N*-terminus of all the peptoids to allow evaluation of their cellular uptake. After deprotection and cleavage from the resin (TFA/TIS/H_2O), the peptoids were purified by semipreparative HPLC and analyzed by MALDI-TOF MS and HPLC (SI, Table S1). The hybrid peptoids were isolated in low yields (5−12%) compared to the other peptoid types, which may be attributed to the aggregation of the peptoid chains in the sterically demanding, resin-bound environment.

Cellular Uptake of Hybrid Peptoids. The cellular uptake of the fluorescein-tagged hybrid peptoids (**H5**, **H7**, **H9**) was evaluated with human embryonic kidney (HEK293T), human cervical carcinoma (HeLa), and Chinese hamster ovary (CHO) cell lines, and compared with the lysine-like peptoids (**L5**, **L7**, **L9**) and TEG peptoids (**T5**, **T7**, **T9**). The cells were incubated with peptoids at 10 μM and analyzed at 2, 4, and 24 h by flow cytometry (Figure 1).

With all peptoid types, the uptake was dependent on the number of monomer units with longer oligomers yielding greater cellular uptake as shown by the fluorescence intensity, which increased over time in a nonlinear manner (with rapid accumulation within the first 4 h), suggesting an active transport mechanism.

A clear difference in the level of uptake was observed with different cells lines, with CHO cells demonstrating notably higher uptake than HeLa and HEK293T with all peptoid types. In HeLa cells, which showed the lowest uptake of the three cell lines, the hybrid nonamer **H9** exhibited the highest cellular uptake, with 4-fold higher fluorescence intensity after 4 h compared to **H7** (Figure 1). After 24 h, a decrease in the fluorescence was observed with the cells incubated with **H9** suggesting saturation of the cells and efflux of **H9** during prolonged incubation, a phenomenon that was not observed with **H5** and **H7**, which exhibited lower initial uptake. Figure 2 shows fluorescent images of HeLa incubated with **H7** at 1 μM. Similarly to HEK293T, **H9** outperformed **L9** and **T9**. Interestingly, with CHO cells, the highest cellular uptake of **H9** was only observed after 24 h of incubation.

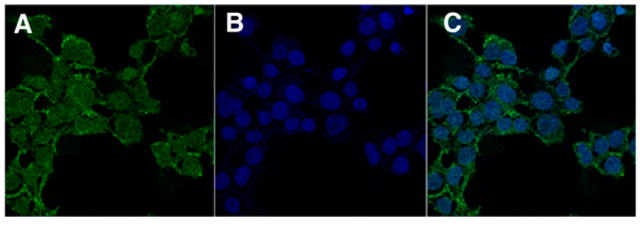

Figure 2. Confocal images of HeLa cells incubated with 1 μM of hybrid peptoid H7 for 12 h. The cells were fixed, nuclei were stained with Hoechst 33342, and the cells imaged (λ_{Ex} 407 nm for Hoechst 33342 and 488 nm for fluorescein). (A) λ_{Ex} 488 nm. (B) λ_{Ex} 407 nm. (C) Composition of fluorescence images at λ_{Ex} 407 and 488 nm.

To better establish the effect of the hybrid structure, the cellular uptake of **H9**, **L9**, and **T9** were directly compared. After 2 h incubation at 1 and 10 μM, the cells were analyzed by flow cytometry. Based on the fluorescence ($\lambda_{Ex}/\lambda_{Em}$ 488/530 nm) intensity of the cells, **H9** showed notably better uptake in all three cell lines at both concentrations when compared to **L9** and **T9** (Figure 3), with **L9** outperforming **T9**. Overall, the hybrid nonamer **H9** was the most efficient peptoid with ∼100% of the cell populations labeled within 2 h at low μM concentrations, whereas TEG-based peptoids exhibited the lowest uptake. The hybrid peptoids **H5**, **H7**, and **H9** were non-cytotoxic, with cell viability ≥96% at 10 μM in PI assays (SI, Figure S3).

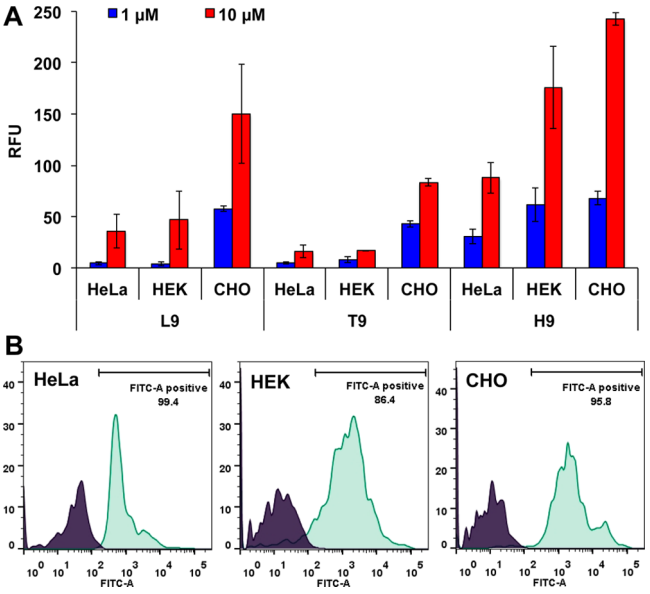

Figure 3. (A) Flow cytometry analysis ($\lambda_{Ex}/\lambda_{Em}$ 488/530 nm) of cellular uptake of nonamer peptoids **L9**, **T9**, and **H9** in HEK293, HeLa, and CHO cells after 2 h incubation at 1 and 10 μM (n = 6). (B) Representative flow cytometry histograms of cells treated with 10 μM of **H9**. Control populations are shown in dark gray, cells treated with **H9** in green (x-axis represents relative fluorescence intensity).

CONCLUSIONS

To enable the efficient solid-phase synthesis of peptoids by the "monomer" approach, a flow-based method for the gram-scale synthesis of peptoid monomers, *N*-Fmoc-(6-Boc-aminohexyl)-glycine and its ethylene glycol analogue *N*-Fmoc-((2-(2-Boc-aminoethoxy)ethoxy)ethyl)glycine, was developed. *N*-Boc monoprotected diamines, synthesized in flow, were selectively *N*-alkylated with benzyl 2-bromoacetate, directly followed by Fmoc carbamation of the secondary amine under flow conditions. Finally, flow transfer hydrogenolysis, using 20% $Pd(OH)_2/C$ as a catalyst and 1,4-cyclohexadiene as the hydrogen donor, resulted in excellent yields of the debenzylated products without notable Fmoc cleavage. This flow procedure offers a continuous mode of processing, which is highly attractive due to its scalability potential, and allows gram-scale access to peptoid monomers. These monomers were used to

DOI: 10.1021/acs.bioconjchem.5b00307
Bioconjugate Chem. XXXX, XXX, XXX−XXX

synthesize a new class hybrid peptoids (5-, 7-, and 9-mers) on solid phase. The fluorescein tagged 9-mer hybrid peptoid **H9**, constructed of alternating units of the aminohexyl and amino-TEG monomers, showed superior cellular uptake on three cell lines when compared to the traditional lysine-like peptoid of the same length. The inability of the peptoids assembled purely from the TEG-based monomer to enhance cellular uptake emphasized the importance of the hybrid structure on transport properties. Their remarkable cellular uptake and non-cytotoxicity highlight the potential of these hybrid peptoids as cellular transporters for biomedical applications.

■ ASSOCIATED CONTENT

Ⓢ Supporting Information

Supporting figures and schemes, and experimental procedures and analytical data for all compounds are included. The Supporting Information is available free of charge on the ACS Publications website at DOI: 10.1021/acs.bioconjchem.5b00307.

■ AUTHOR INFORMATION

Corresponding Author

*E-mail: mark.bradley@ed.ac.uk.

Notes

The authors declare no competing financial interest.

■ ACKNOWLEDGMENTS

We thank the MTEM School of Chemistry Studentship for funding TSJ, Caja Madrid and Ramon Areces Foundation for funding AMPL, and University of Edinburgh (Innovation Initiative Grant) for financial support.

■ REFERENCES

(1) Allen, T. M., and Cullis, P. R. (2004) Drug delivery systems: Entering the mainstream. *Science 303*, 1818−1822.

(2) Reischl, D., and Zimmer, A. (2009) Drug delivery of siRNA therapeutics: potentials and limits of nanosystems. *Nanomedicine 5*, 8−20.

(3) Shin, M. C., Zhang, J., Min, K. A., Lee, K., Byun, Y., David, A. E., He, H., and Yang, V. C. (2014) Cell-penetrating peptides: Achievements and challenges in application for cancer treatment. *J. Biomed. Mater. Res., Part A 102*, 575−587.

(4) Tuma, P. L., and Hubbard, A. L. (2003) Transcytosis: Crossing cellular barriers. *Physiol. Rev. 83*, 871−932.

(5) Diao, L., and Meibohm, B. (2013) Pharmacokinetics and pharmacokinetic-pharmacodynamic correlations of therapeutic peptides. *Clin. Pharmacokinet. 52*, 855−868.

(6) Murphy, J. E., Uno, T., Hamer, J. D., Cohen, F. E., Dwarki, V., and Zuckermann, R. N. (1998) A combinatorial approach to the discovery of efficient cationic peptoid reagents for gene delivery. *Proc. Natl. Acad. Sci. U. S. A. 95*, 1517−1522.

(7) Xu, Z. P., Zeng, Q. H., Lu, G. Q., and Yu, A. B. (2006) Inorganic nanoparticles as carriers for efficient cellular delivery. *Chem. Eng. Sci. 61*, 1027−1040.

(8) Vasir, J. K., and Labhasetwar, V. (2007) Biodegradable nanoparticles for cytosolic delivery of therapeutics. *Adv. Drug Delivery Rev. 59*, 718−728.

(9) Wang, F., Wang, Y., Zhang, X., Zhang, W., Guo, S., and Jin, F. (2014) Recent progress of cell-penetrating peptides as new carriers for intracellular cargo delivery. *J. Controlled Release 174*, 126−136.

(10) Stewart, K. M., Horton, K. L., and Kelley, S. O. (2008) Cell-penetrating peptides as delivery vehicles for biology and medicine. *Org. Biomol. Chem. 6*, 2242−2255.

(11) Foerg, C., and Merkle, H. P. (2008) On the biomedical promise of cell penetrating peptides: Limits versus prospects. *J. Pharm. Sci. 97*, 144−162.

(12) Weeks, B. S., Desai, K., Loewenstein, P. M., Klotman, M. E., Klotman, P. E., Green, M., and Kleinman, H. K. (1993) Identification of a novel cell attachment domain in the HIV-1 Tat protein and its 90-kDa cell surface binding protein. *J. Biol. Chem. 268*, 5279−5284.

(13) Debaisieux, S., Rayne, F., Yezid, H., and Beaumelle, B. (2012) The Ins and Outs of HIV-1 Tat. *Traffic 13*, 355−363.

(14) Derossi, D., Chassaing, G., and Prochiantz, A. (1998) Trojan peptides: the penetratin system for intracellular delivery. *Trends Cell Biol. 8*, 84−87.

(15) Pooga, M., Hällbrink, M., Zorko, M., and Langel, Ü. (1998) Cell penetration by transportan. *FASEB J. 12*, 67−77.

(16) Foerg, C., Ziegler, U., Fernandez-Carneado, J., Giralt, E., Rennert, R., Beck-Sickinger, A. G., and Merkle, H. P. (2005) Decoding the entry of two novel cell-penetrating peptides in HeLa Cells: Lipid raft-mediated endocytosis and endosomal escape. *Biochemistry 44*, 72−81.

(17) Jiao, C.-Y., Delaroche, D., Burlina, F., Alves, I. D., Chassaing, G., and Sagan, S. (2009) Translocation and endocytosis for cell-penetrating peptide internalization. *J. Biol. Chem. 284*, 33957−33965.

(18) Madani, F., Lindberg, S., Langel, Ü., Futaki, S., and Gräslund, A. (2011) Mechanisms of cellular uptake of cell-penetrating peptides. *J. Biophys. 2011*, 1−10.

(19) Ryser, H. J. P., and Shen, W.-C. (1978) Conjugation of methotrexate to poly(L-lysine) increases drug transport and overcomes drug resistance in cultured cells. *Proc. Natl. Acad. Sci. U. S. A. 75*, 3867−3870.

(20) Rothbard, J. B., Garlington, S., Lin, Q., Kirschberg, T., Kreider, E., McGrane, P. L., Wender, P. A., and Khavari, P. A. (2000) Conjugation of arginine oligomers to cyclosporin A facilitates topical delivery and inhibition of inflammation. *Nat. Med. 6*, 1253−1257.

(21) Wender, P. A., Mitchell, D. J., Pattabiraman, K., Pelkey, E. T., Steinman, L., and Rothbard, J. B. (2000) The design, synthesis, and evaluation of molecules that enable or enhance cellular uptake: Peptoid molecular transporters. *Proc. Natl. Acad. Sci. U. S. A. 97*, 13003−13008.

(22) Mitchell, D. J., Steinman, L., Kim, D. T., Fathman, C. G., and Rothbard, J. B. (2000) Polyarginine enters cells more efficiently than other polycationic homopolymers. *J. Pept. Res. 56*, 318−325.

(23) Simon, R. J., Kania, R. S., Zuckermann, R. N., Huebner, V. D., Jewell, D. A., Banville, S., Ng, S., Wang, L., Rosenberg, S., and Marlowe, C. K. (1992) Peptoids: a modular approach to drug discovery. *Proc. Natl. Acad. Sci. U. S. A. 89*, 9367−9371.

(24) Peretto, I., Sanchez-Martin, R. M., Wang, X. H., Ellard, J., Mittoo, S., and Bradley, M. (2003) Cell penetrable petoid carrier vehicles: synthesis and evaluation. *Chem. Commun.*, 2312−2313.

(25) Chongsiriwatana, N. P., Patch, J. A., Czyzewski, A. M., Dohm, M. T., Ivankin, A., Gidalevitz, D., Zuckermann, R. N., and Barron, A. E. (2008) Peptoids that mimic the structure, function, and mechanism of helical antimicrobial peptides. *Proc. Natl. Acad. Sci. U. S. A. 105*, 2794−2799.

(26) Diaz-Mochon, J. J., Fara, M. A., Sanchez-Martin, R. M., and Bradley, M. (2008) Peptoid dendrimers - Microwave-assisted solid-phase synthesis and transfection agent evaluation. *Tetrahedron Lett. 49*, 923−926.

(27) Zuckermann, R. N., and Kodadek, T. (2009) Peptoids as potential therapeutics. *Curr. Opin. Mol. Ther. 11*, 299−307.

(28) Chen, X., Wu, J., Luo, Y., Liang, X., Supnet, C., Kim, M. W., Lotz, G. P., Yang, G., Muchowski, P. J., Kodadek, T., and Bezprozvanny, I. (2011) Expanded polyglutamine-binding peptoid as a novel therapeutic agent for treatment of Huntington's disease. *Chem. Biol. 18*, 1113−1125.

(29) Tan, N. C., Yu, P., Kwon, Y.-U., and Kodadek, T. (2008) High-throughput evaluation of relative cell permeability between peptoids and peptides. *Bioorg. Med. Chem. 16*, 5853−5861.

(30) Fowler, S. A., and Blackwell, H. E. (2009) Structure-function relationships in peptoids: Recent advances toward deciphering the

DOI: 10.1021/acs.bioconjchem.5b00307
Bioconjugate Chem. XXXX, XXX, XXX−XXX

structural requirements for biological function. *Org. Biomol. Chem. 7*, 1508−1524.
(31) Dhaliwal, K., Alexander, L., Escher, G., Unciti-Broceta, A., Jansen, M., Mcdonald, N., Cardenas-Maestre, J.-M., Sanchez-Martin, R., Simpson, J., Haslett, C., et al. (2011) Multi-modal molecular imaging approaches to detect primary cells in preclinical models. *Faraday Discuss. 149*, 107−114.
(32) Kumar, P., Fara, M. A., Bradley, M., Friedmann, P. S., and Healy, E. (2006) Peptoid modification of alpha-melanocyte stimulating hormone to enhance penetration into skin. *Br. J. Dermatol. 155*, 231−259 Abstracts of the British Society for Investigative Dermatology Annual Meeting, Manchester, April 10-12, 2006.
(33) Schröder, T., Schmitz, K., Niemeier, N., Balaban, T. S., Krug, H. F., Schepers, U., and Bräse, S. (2007) Solid-phase synthesis, bioconjugation, and toxicology of novel cationic oligopeptoids for cellular drug delivery. *Bioconjugate Chem. 18*, 342−354.
(34) Unciti-Broceta, A., Diezmann, F., Ou-Yang, C. Y., Fara, M. A., and Bradley, M. (2009) Synthesis, penetrability and intracellular targeting of fluorescein-tagged peptoids and peptide-peptoid hybrids. *Bioorg. Med. Chem. 17*, 959−966.
(35) Kruijtzer, J. A. W., Hofmeyer, L. J. F., Heerma, W., Versluis, C., and Liskamp, R. M. J. (1998) Solid-phase syntheses of peptoids using Fmoc-Protected *N*-substituted glycines: The synthesis of (retro)-peptoids of leu-enkephalin and substance P. *Chem. - Eur. J. 4*, 1570−1580.
(36) Wegner, J., Ceylan, S., and Kirschning, A. (2012) Flow chemistry − A key enabling technology for (multistep) organic synthesis. *Adv. Synth. Catal. 354*, 17−57.
(37) Yoshida, J.-i., Nagaki, A., and Yamada, D. (2013) Continuous flow synthesis. *Drug Discovery Today: Technol. 10*, e53−e59.
(38) Wiles, C., and Watts, P. (2014) Continuous process technology: A tool for sustainable production. *Green Chem. 16*, 55−62.
(39) Webb, D., and Jamison, T. F. (2010) Continuous flow multi-step organic synthesis. *Chem. Sci. 1*, 675−680.
(40) O'Brien, A. G., Horváth, Z., Lévesque, F., Lee, J. W., Seidel-Morgenstern, A., and Seeberger, P. H. (2012) Continuous synthesis and purification by direct coupling of a flow reactor with simulated moving-bed chromatography. *Angew. Chem., Int. Ed. 51*, 7028−7030.
(41) Simon, M. D., Heider, P. L., Adamo, A., Vinogradov, A. A., Mong, S. K., Li, X., Berger, T., Policarpo, R. L., Zhang, C., Zou, Y., et al. (2014) Rapid flow-based peptide synthesis. *ChemBioChem 15*, 713−720.
(42) Snead, D. R., and Jamison, T. F. (2015) A three-minute synthesis and purification of ibuprofen: Pushing the limits of continuous-flow processing. *Angew. Chem., Int. Ed. 54*, 983−987.
(43) Talla, A., Driessen, B., Straathof, N. J. W., Milroy, L.-G., Brunsveld, L., Hessel, V., and Noël, T. (2015) Metal-free photocatalytic aerobic oxidation of thiols to disulfides in batch and continuous-flow. *Adv. Synth. Catal.*, n/a.
(44) Kockmann, N., Gottsponer, M., Zimmermann, B., and Roberge, D. M. (2008) Enabling continuous-flow chemistry in microstructured devices for pharmaceutical and fine-chemical production. *Chem. - Eur. J. 14*, 7470−7477.
(45) Hartman, R. L., McMullen, J. P., and Jensen, K. F. (2011) Deciding whether to go with the flow: Evaluating the merits of flow reactors for synthesis. *Angew. Chem., Int. Ed. 50*, 7502−7519.
(46) Su, Y., Straathof, N. J. W., Hessel, V., and Noël, T. (2014) Photochemical transformations accelerated in continuous-flow reactors: Basic concepts and applications. *Chem. - Eur. J. 20*, 10562−10589.
(47) Jong, T., and Bradley, M. (2015) Flow-mediated synthesis of Boc, Fmoc, and Ddiv monoprotected diamines. *Org. Lett. 17*, 422−425.
(48) Huang, W., Seo, J., Lin, J. S., and Barron, A. E. (2012) Peptoid transporters: Effects of cationic, amphipathic structure on their cellular uptake. *Mol. BioSyst. 8*, 2626−2628.
(49) Vollrath, S. B. L., Fürniss, D., Schepers, U., and Bräse, S. (2013) Amphiphilic peptoid transporters - synthesis and evaluation. *Org. Biomol. Chem. 11*, 8197−8201.
(50) Martin, E. J., Blaney, J. M., Siani, M. A., Spellmeyer, D. C., Wong, A. K., and Moos, W. H. (1995) Measuring diversity: Experimental design of combinatorial libraries for drug discovery. *J. Med. Chem. 38*, 1431−1436.
(51) Combs, D. J., and Lokey, R. S. (2007) Extended peptoids: A new class of oligomers based on aromatic building blocks. *Tetrahedron Lett. 48*, 2679−2682.
(52) Kölmel, D. K., Hörner, A., Rönicke, F., Nieger, M., Schepers, U., and Bräse, S. (2014) Cell-penetrating peptoids: Introduction of novel cationic side chains. *Eur. J. Med. Chem. 79*, 231−243.
(53) Gajbhiye, V., Vijayaraj Kumar, P., Tekade, R. K., and Jain, N. K. (2007) Pharmaceutical and biomedical potential of PEGylated dendrimers. *Curr. Pharm. Des. 13*, 415−429.
(54) Fox, M. E., Guillaudeu, S., Fréchet, J. M. J., Jerger, K., Macaraeg, N., and Szoka, F. C. (2009) Synthesis and in vivo antitumor efficacy of PEGylated poly(l-lysine) dendrimer-camptothecin conjugates. *Mol. Pharmaceutics 6*, 1562−1572.
(55) Fant, K., Esbjörner, E. K., Jenkins, A., Grossel, M. C., Lincoln, P., and Nordén, B. (2010) Effects of PEGylation and acetylation of PAMAM dendrimers on DNA binding, cytotoxicity and in vitro transfection efficiency. *Mol. Pharmaceutics 7*, 1734−1746.
(56) Martinez, J., Tolle, J. C., and Bodanszky, M. (1979) Side reactions in peptide synthesis. 12. Hydrogenolysis of the 9-fluorenylmethyloxycarbonyl group. *J. Org. Chem. 44*, 3596−3598.
(57) Atherton, E., Bury, C., Sheppard, R. C., and Williams, B. J. (1979) Stability of fluorenylemthoxycarbonylamino groups in peptide synthesis. Cleavage by hydrogenolysis and by dipolar aprotic solvent. *Tetrahedron Lett. 20*, 3041−3042.
(58) Thakkar, A., Cohen, A. S., Connolly, M. D., Zuckermann, R. N., and Pei, D. (2009) High-throughput sequencing of peptoids and peptide-peptoid hybrids by partial Edman degradation and mass spectrometry. *J. Comb. Chem. 11*, 294−302.
(59) Bensel, N., Klär, D., Catala, C., Schneckenburger, P., Hoonakker, F., Goncalves, S., and Wagner, A. (2010) A chemometric approach to map reaction media chemoselectivity: Example of selective debenzylation. *Eur. J. Org. Chem. 2010*, 2261−2264.

DOI: 10.1021/acs.bioconjchem.5b00307
Bioconjugate Chem. XXXX, XXX, XXX−XXX